Cement & Concrete Composites 37 (2013) 259–266

Contents lists available at SciVerse ScienceDirect

Cement & Concrete Composites

journal homepage: www.elsevier.com/locate/cemconcomp

Freeze–thaw resistance and transport properties of high-volume fly ash roller compacted concrete designed by maximum density method

Ali Mardani-Aghabaglou *, Özge Andiç-Çakir, Kambiz Ramyar

Department of Civil Engineering, Eng. Faculty, Ege University, Bornova-İzmir, Turkey

ARTICLE INFO

Article history:
Received 5 November 2012
Received in revised form 4 January 2013
Accepted 5 January 2013
Available online 24 January 2013

Keywords:
Roller compacted concrete
Fly ash
Durability
Maximum density method

ABSTRACT

The aim of this study is to evaluate the effect of high-volume fly ash on some durability characteristics of roller compacted concrete (RCC). In addition to a control mixture without fly ash, two different series of mixtures were prepared by partial replacement of either cement or aggregate with fly ash. The mixtures were designed by a maximum density method. A total of 28 mixtures having four different water/binder ratios (0.30, 0.35, 0.40 and 0.45 by mass) were prepared to determine the optimum water/binder ratio. Among these, seven mixtures containing the optimum water content were selected for further experimental study. It was observed that in the mixtures where cement was substituted with fly ash, increasing the fly ash content adversely affected the durability performance up to 90 days. However, fly ash substitution for a part of the aggregate improved the durability characteristics of the mixture as the amount of fly ash increased.

1. Introduction

The effects of high-volume fly ash on the mechanical properties of hardened roller compacted concrete (RCC) have been discussed previously [1]. Roller compacted concrete (RCC) is a no-slump concrete obtained by using similar materials to those of conventional concrete, however, containing a relatively lower binder content than normal concrete [2–6]. RCC mixtures can be designed by using a maximum density method or a concrete method [7,8]. RCC is preferred due to its cost efficiency, low heat of hydration, and quick and easy application in concrete gravity dams, airport runways and concrete pavements [9,10].

In cold climates, damage to concrete pavements, retaining walls, bridge decks and railings exposed to frost action is one of the major problems requiring heavy expenditures for the repair and replacement of structures. Frost damage in concrete can take several forms. The most common damage is cracking and spalling of concrete caused by progressive expansion of the cement paste matrix from repeated freezing and thawing cycles. It is reported that saturated non-air entrained RCC shows unsatisfactory performance upon exposure to freeze–thaw; however, in a non-saturated state, the frost resistance of RCC is satisfactory [11]. Durability characteristics and transport properties of RCC mixtures were studied by several investigators [12–17]. The durability of concrete depends, to a large extent, on its water permeability and diffusivity. Permeability is defined as the property that governs the rate of flow of a fluid into a porous material under pressure. The permeability of concrete can be measured by determining the rate of water flow under pressure through the concrete. The porosity in concrete can largely affect the permeability. A large amount of porosity in concrete resides at the interface between the aggregate and the cement paste [11,18]. Transport properties of high volume fly ash roller compacted concrete have been investigated by Amarnath and Ganesh Babu [10]. Their results showed that RCCs of moderate cement and moderate fly ash contents had lower values of water permeability, absorption, sorptivity and chloride penetration than the control mixture. Nili and Zaheri [19] showed that the natural pozzolans were effective in reducing the salt-scaling resistance of RCC. Salt scaling decreased as the duration of the freeze period in the freeze–thaw cycle decreased. The influence of mixture composition on strength and freeze–thaw resistance of RCC was investigated by Hazaree et al. [20]. In this study, RCC mixtures containing a wide range of cement contents between 100 and 450 kg/m^3 were investigated. Significant differences between the physical and mechanical properties of RCC and traditional concrete mixtures were observed. Air entrainment was found to improve effectively both the strength and freeze–thaw resistance of RCC mixtures. Gao et al. [21] investigated the freeze–thaw resistance of fly ash incorporating RCC mixtures with a total binder content of 200 kg/m^3. The linear relationship between mass loss and strength loss of RCC mixtures was found to be similar to that of traditional concrete. However, the spacing factor to obtain a reasonable freeze–thaw resistance was found to be less than 0.4 mm, for RCC mixtures. Another investigation by Ghafoori and Yuzheng

* Corresponding author. Tel.: +90 232 3886026; fax: +90 232 3425629.
E-mail address: ali.mardani16@gmail.com (A. Mardani-Aghabaglou).

0958-9465/$ - see front matter © 2013 Elsevier Ltd. All rights reserved.
http://dx.doi.org/10.1016/j.cemconcomp.2013.01.009

[22] indicates that a maximum mass loss of 2.3% and minimum durability factor of 91.2% can be reached on RCC samples containing high calcium dry bottom ash after 300 rapid freeze–thaw cycles.

Fly ash is used as a cement replacement material in several special types of concrete such as RCC, self-compacting reactive-powder concrete, and lightweight concrete [23–30]. However, there is a lack of study related with replacement of aggregate with fly ash in RCC mixtures. In this study, the effect of high-volume fly ash on some durability characteristics of RCC mixtures such as water absorption, water sorptivity, permeable void content, determination of depth of penetration of water under pressure, dynamic modulus of elasticity and freeze–thaw resistance, where a part of either cement or aggregate was replaced with fly ash, were investigated.

2. Materials and methods

2.1. Materials

In this study, a CEM I 42.5 R type cement conforming to EN 197-1 standard [31] and a high-lime fly ash conforming to the EN 450-1 standard were used [32] as binders. The chemical compositions, as well as some mechanical and physical properties of the cement and fly ash obtained from their manufacturers, are given in Table 1. The specific gravity and water absorption capacity of the aggregates used in the experiments were determined in accordance with the EN 1097-6 standard [33]. The saturated-surface-dry (SSD) specific gravities of 0–5 mm, 5–15 mm and 15–25 mm aggregate size fractions were obtained as 2.60, 2.65 and 2.67 respectively, and the loose bulk densities of these size fractions were 1740, 1505 and 1480 kg/m^3, respectively. The gradation of combined aggregate, obtained by mixing 60% 0–5 mm, 20% 5–15 mm and 20% 15–25 mm aggregate size fractions by mass, and the standard gradation limits are shown in Fig. 1 [34].

2.2. Methods

The experimental study was performed in two stages:

(a) Determination of the optimum water content of the mixtures: the optimum water contents of the control mixture and the RCCs containing fly ash were determined. In this stage, 28 different mixtures were prepared and among these, seven mixtures having optimum water content were selected for further studies.
(b) Determination of durability characteristics: the 56-day water absorption, water sorptivity, permeable void content, depth of penetration of water under pressure, dynamic modulus of elasticity and 90-day freeze–thaw resistance of the selected seven RCC mixtures were investigated.

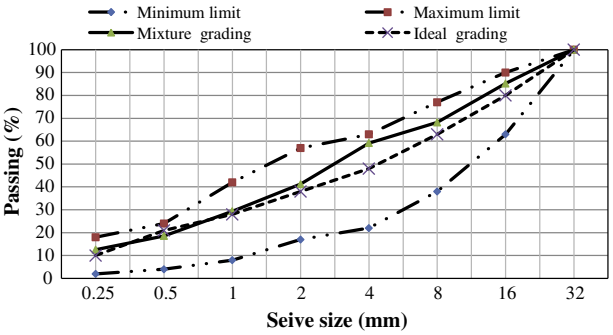

Fig. 1. Gradation curve of combined aggregate and TS 802 standard limits.

2.2.1. Determination of optimum water content

The mixtures used in the experimental study were designed according to the maximum density method in accordance with ACI 207.5R.89 [35]. The cement content of the control mixture was 250 kg/m^3. RCC mixtures were prepared by replacing 20, 40 and 60 wt.% of cement with fly ash, respectively. Three other series were prepared by replacing a part of the aggregate with fly ash. The substitution levels of aggregate with fly ash were 20, 40 and 60 wt.% of cement, respectively. Using four different water/binder (w/b) ratios i.e. 0.30, 0.35, 0.40 and 0.45, 28 RCC mixtures were prepared and cast into 150 × 300 mm cylindrical molds in three layers in accordance with the ASTM C 1435 standard [36]. A 5 kg steel compacting plate shown in Fig. 2 was used to homogeneously distribute the load applied by a vibrating hammer and to obtain a smooth surface during compaction of each layer. A maximum 20 s vibration period was used for each layer.

In order to obtain the optimum water content of each mixture, samples were taken from the compacted specimens and dried in an electrical oven at 105 °C to a constant mass. The water content (w) was calculated according to following equation:

$$w = \frac{m_{wet} - m_{dry}}{m_{dry}} \times 100 \quad (1)$$

where m_{wet} is the mass of wet specimen (g), m_{dry} is the mass of oven dry specimen (g).

The wet unit weight (γ_{wet}) was obtained by dividing the mass of wet concrete specimen (m) into its volume (v) [37]. The dry unit weight (γ_{dry}) was calculated by dividing the wet unit weight into one plus the measured water content as shown in following equation:

$$\gamma_{dry} = \frac{\gamma_{wet}}{1 + w} \quad (2)$$

The relationship between water content and dry unit weight for each mixture was plotted. From the resultant curve, the optimum water content corresponding to the maximum dry unit weight was

Table 1
Chemical composition, mechanical and physical properties of cement and fly ash.

Chemical properties			Mechanical and physical properties			
Oxide (%)	Cement	Fly ash	Properties		Cement	Fly ash
SiO_2	18.53	49.70	Compressive strength (MPa)	2 Day	24.3	–
Al_2O_3	5.01	17.01		7 Day	39.9	–
Fe_2O_3	2.74	8.87		28 Day	47.0	
CaO	63.51	10.88	Specific gravity	–	3.13	2.28
MgO	1.06	5.95	Strength activity index (%)	7 Day	–	81
Na_2O	0.40	1.66		28 Day	–	87
K_2O	0.75	1.30	Fineness	Blaine specific surface (cm^2/g)	3880	4040
SO_3	3.14	2.52		Residual of 0.090 mm sieve (%)	1.0	5.3
				Residual of 0.032 mm sieve (%)	22.4	16.5

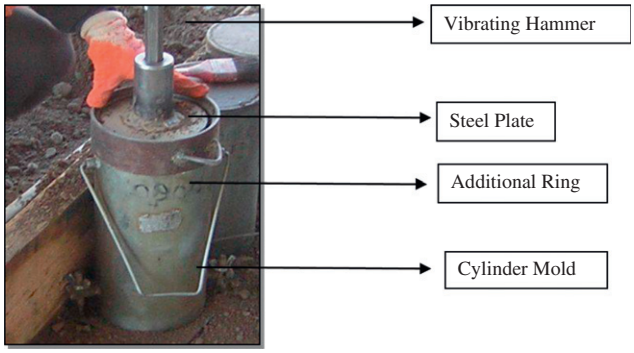

Fig. 2. Additional ring and steel plate used during the production of specimens.

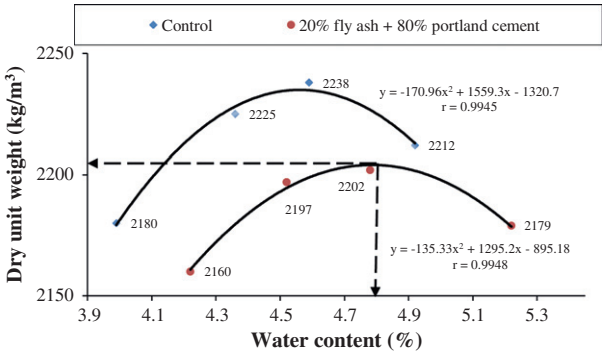

Fig. 3. Relation between water content and maximum dry unit weight of control mixture and fly ash replaced with 20% by weight cement – determination of optimum water content.

determined as shown in Fig. 3. The results are given in Table 2. Those mixtures where cement is partially replaced with fly ash are designated as series A, whereas those mixtures in which aggregate is partially substituted with fly ash are designated as series B.

The mixture proportions of the concrete mixtures are given in Table 3. As it can be seen from Table 3, since the optimum water content of the fly ash – bearing mixtures is higher than that of the control mixture, w/b ratios of the fly ash RCC mixtures are greater than that of control mixture. The effect is more pronounced in the mixtures containing a higher amount of fly ash.

The specimens were prepared and demolded 24 h after casting and then stored in 23 ± 2 °C water for curing until reaching their testing age, which was denoted in this study as XX-days.

3. Test procedures

3.1. Water absorption and permeable void content

The 56-day water absorption and permeable void content of 150 mm cube specimens were obtained in accordance with the ASTM C 642-97 [38] standard. Saturated surface dry specimens were weighed (b) and then kept in an oven maintained at 100–110 °C until a constant mass (a) was attained. The specimens were placed in a suitable receptacle, covered with tap water, and boiled for 5 h. Then, they were allowed to cool to room temperature (22 ± 2 °C). The surface moisture was removed with a towel and the surface-dried mass of the boiled specimens (c) was determined. The immersed apparent mass (d) of both boiled and unboiled specimens were determined in water. Absorption after immersion (m_1), and absorption after immersion and boiling (m_2) as well as their permeable void content (B_0) were calculated according to Eqs. (3)–(5), respectively.

$$m_1 = [(b - a)/a] \times 100 \quad (3)$$

$$m_2 = [(c - a)/a] \times 100 \quad (4)$$

$$B_0 = [(c - a)/(c - d)] \times 100 \quad (5)$$

3.2. Determination of depth of penetration of water under pressure and unit weight determination

The 56-day permeability and unit weight of 150 mm cube specimens were obtained in accordance with the EN 12390-8 [39] and EN 12390-7 [40] standards, respectively.

Table 2
Optimum water content, maximum dry unit weight and water/binder ratio of the mixtures.

RCC mix no		Optimum water content (%)	Maximum dry unit weight (kg/m³)	w/b Ratio	Water content for 1 m³ RCC (kg)
C	Control	4.58	2232	0.39	97.5
A1[a]	80 PC + 20 FA	4.78	2205	0.40	100
A2	60 PC + 40 FA	5.60	2129	0.42	105
A3	40 PC + 60 FA	6.10	2078	0.46	115
B1[a]	100 PC + 20 FA	4.90	2228	0.41	123
B2	100 PC + 40 FA	5.74	2125	0.43	150.5
B3	100 PC + 60 FA	6.16	2056	0.47	188

[a] In series A Portland cement (PC) was partially substituted with fly ash (FA) and in series B aggregate was partially replaced with fly ash.

Table 3
Mix proportions of the RCC mixtures.

Mixture	Cement (kg/m³)	Fly ash (kg/m³)	SSD aggregate			Water (kg/m³)	Water/binder ratio
			0–5 mm (kg/m³)	5–15 mm (kg/m³)	15–25 mm (kg/m³)		
C	250	0	1263	429	432	97.5	0.39
A1	200	50	1248	424	427	100	0.40
A2	150	100	1235	419	422	105	0.42
A3	100	150	1209	410	413	115	0.46
B1	250	50	1185	402	405	123	0.41
B2	250	100	1107	376	379	150.5	0.43
B3	250	150	1020	346	349	188	0.47

3.3. Sorptivity test

The sorptivity test (ASTM C 1585 with modifications provided below) [41] was performed on 150 mm cube specimens. For this aim, the 56-day specimens were dried at 105 °C until reaching a constant mass, as opposed to the pre-conditioning regimen outlined in the ASTM standard, and then the side surfaces of the cubes were sealed with an acrylic copolymer-based sealing material. Supporting rods were placed at the bottom of the pan and the pan was filled with tap water to a level of 1–3 mm above the top of the supporting rods. At target times (0, 5, 10, 20, 30, 60, 120, 180, 240, 300, 360, 1440, 2880, 4320 min), the mass of the specimens was measured, and then the change in specimen mass was determined. The sorptivity was calculated according to following equation:

$$I = \frac{m_t}{a \times d} \tag{6}$$

where I is the sorptivity (mm), m_t the change in specimen mass (g), a the exposed area of the specimen (mm^2), and d is the density of the water (g/mm^3).

3.4. Determination of dynamic elastic modulus by ultrasonic pulse velocity (UPV)

The UPV values of 90-day old concrete mixtures were determined on 150 mm cube specimens in accordance with the ASTM C 597 [42] standard. The dynamic elastic modulus of 150 mm cube specimens was calculated by Eq. (7) [43,44]:

$$E_{dn} = \rho c^2 \frac{(1+\nu)(1-2\nu)}{(1-\nu)} \tag{7}$$

where E_{dn} is the dynamic elastic modulus of concrete (MPa), ρ the hardened concrete density (kg/m^3), c the UPV (km/s) and ν is the Poisson's ratio. Poisson's ratio was assumed as 0.2 for all concrete mixtures.

3.5. Freeze–thaw resistance

The 90-day freeze–thaw resistance of hardened concrete mixtures was determined on three 150 mm cube specimens in accordance with the ASTM C666/C666M – 03 [45] standard. The concrete specimens were frozen in air from 5 ± 2 °C to −18 ± 2 °C within 3 h and were thawed in water to 5 ± 2 °C within 1 h in a single cycle. The changes in weight and dynamic modulus of elasticity of each specimen were measured at every 30 freeze–thaw cycles until 300 cycles. The changes in weight of the cube specimens (W) were calculated using Eq. (8) given in TS 3699 [46]. Furthermore, their durability factor (D_f) was determined using Eq. (9) proposed by Neville [43].

$$W = [(W_2 - W_1)/W_1)] \times 100 \tag{8}$$

$$D_f = \frac{n}{3}\left[\frac{E_{dn}}{E_{d0}}\right] \tag{9}$$

where W_1 is the weight of specimen at the beginning of test (g), W_2 the weight of specimen after n cycles (g), E_{dn} the dynamic modulus at the end of n = 300 cycles (MPa) and E_{d0} is the dynamic modulus at the beginning of the test (MPa). The value of D_f is primarily of interest in the comparison of different concrete mixtures, preferably when only one variable (such as aggregate) is changed. The value of D_f smaller than 40 indicates that the concrete is probably unsatisfactory, values between 40 and 60 are regarded as doubtful, while values over 60 indicate that the concrete is likely satisfactory [43].

4. Results and discussion

4.1. Water absorption and permeable void content

The absorption values after immersion (m_1), after immersion and boiling (m_2) and the permeable void contents of the RCC mixtures are given in Figs. 4 and 5, respectively. Each value represents the average of three measurements. It can be seen that the water absorption values of all RCC mixtures are lower than 3%, the limit specified for good concrete in accordance with CEB-FIP [47].

As expected, permeable void and water absorption values increase by increasing fly ash replacement level of the series A mixtures compared to those of the control mixture. However, in series B, permeable void and water absorption values were decreased by increasing fly ash content. The measured void content in these series are not only the capillary pores but also the entrapped air of the mixtures. Thus, the influence of compactability on the void content is more pronounced than that of w/b ratio. In addition, the absorption values after immersion (m_1) are lower than those after immersion and boiling (m_2). This may be attributed to the probable increase in aggregate–cement paste interfacial transition zone (ITZ) cracks and removal of some entrapped air from the specimens during boiling. As shown in Fig. 6, a strong linear relationship between water absorption and permeable void content of the mixtures were obtained.

4.2. Penetration of water under pressure

The two important factors determining the permeability of concrete are the entrapped air content and the capillary porosity of the

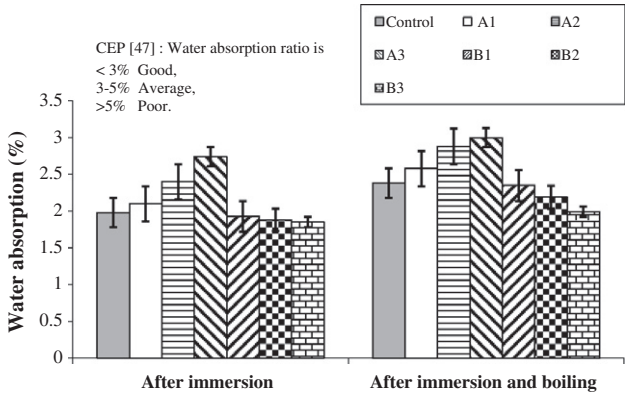

Fig. 4. Water absorption values of RCC mixtures after immersion (m_1) and after immersion and boiling (m_2).

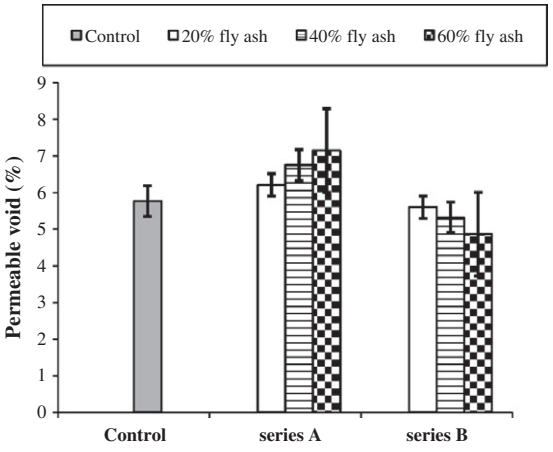

Fig. 5. Permeable void contents of RCC mixtures.

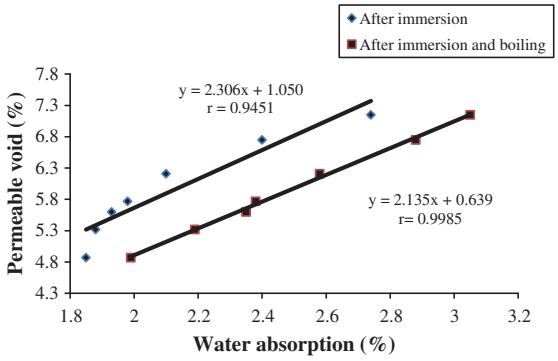

Fig. 6. Relationship between permeable void content and water absorption.

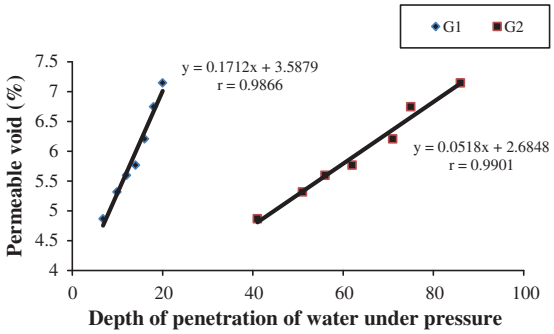

Fig. 8. Relationship between water permeability and permeable void content of RCC mixtures, G_1: tested perpendicular to the casting layers, G_2: tested parallel to the casting layers.

hydrated cement matrix [48]. In this study, the permeability of concrete was measured in two directions; G_1: perpendicular to the casting layers and G_2: parallel to the casting layers of the specimen. The latter characteristic is of importance in dam construction, where the cold joints between the layers are parallel to the casting layers. The values of depth of penetration of water under pressure are given in Fig. 7. Each value represents the average of three measurements. As it was expected, regardless of the type of the mixture, G_2 values are always significantly greater than the corresponding G_1 values. The strong relationship between permeable void content and depth of water under pressure for the G_1 and G_2 series is shown in Fig. 8. It is seen that in series A, depth of penetration of water under pressure (for both G_1 and G_2) increased with increasing fly ash content compared to that of control mixture. However in series B, depth of penetration of water under pressure (for both G_1 and G_2) decreased with increasing fly ash content compared to that of the control.

4.3. Sorptivity

The 56-day sorptivity test results of RCC mixtures are shown in Fig. 9. Each value represents the average of three measurements. It can be seen that compared to the control mixture, the sorptivity values were increased for series A and decreased for series B as the replacement level of fly ash increased. The relationship between permeability of G_1 and G_2 test series and their sorptivity values are given in Fig. 10. Each value represents the average of three measurements. As expected, a strong linear relationship was obtained between permeability and sorptivity values of the various RCC mixtures.

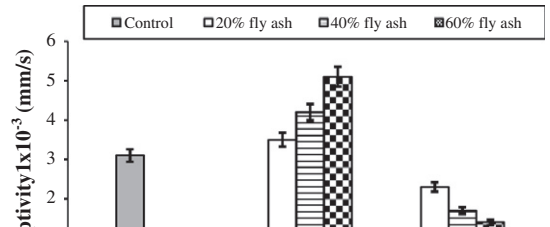

Fig. 9. Sorptivity values of RCC mixtures.

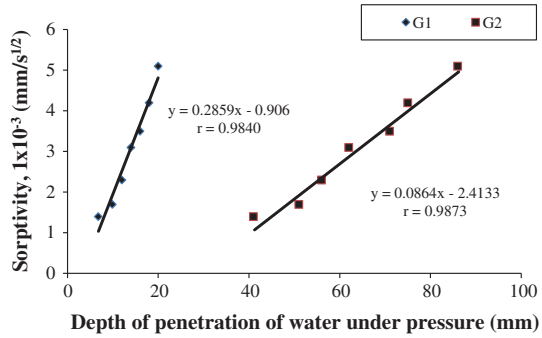

Fig. 10. Relationship between permeability and sorptivity values of RCC mixtures, G_1: tested perpendicular to the casting layers, G_2: tested parallel to the casting layers.

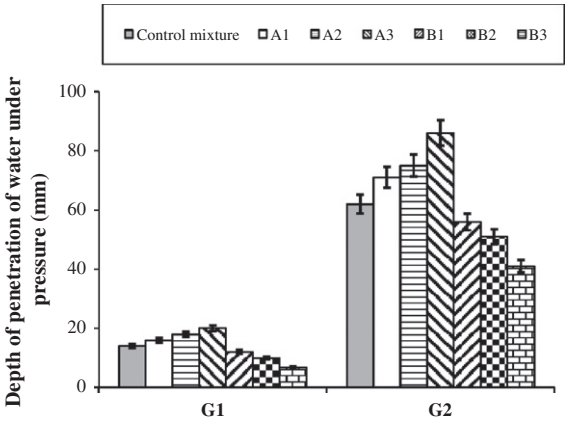

Fig. 7. Depth of penetration of water under pressure of RCC mixtures, G_1: tested perpendicular to the casting layers, G_2: tested parallel to the casting layers.

The maximum and minimum permeable void content, water absorption, depth of penetration of water under pressure (G_1 and G_2) and sorptivity results belong to the A3 and B3 mixtures, respectively. In the A3 and B3 mixtures, a part of cement and aggregate (equal to 60 wt.% of cement) was replaced with fly ash, respectively. In series B3, the binder content of the mixture rose from 250 kg/m^3 to 400 kg/m^3. Meanwhile, due to an increase in the optimum water content upon fly ash substitution, the w/b ratio of the mixture was increased to 0.47 which is considerably higher than that of control mixture (0.39). However, in spite of having a greater w/b ratio, the B3 mixture showed the best transport properties. The increase in above mentioned characteristics in series A may be attributed to the increase in w/b ratio as well as the porosity of series A mixtures by increasing the fly ash replacement level. However, contradictory characteristics of series B – improving transport properties by increasing replacement level of fly ash – may be due to achieving better compactability upon increasing

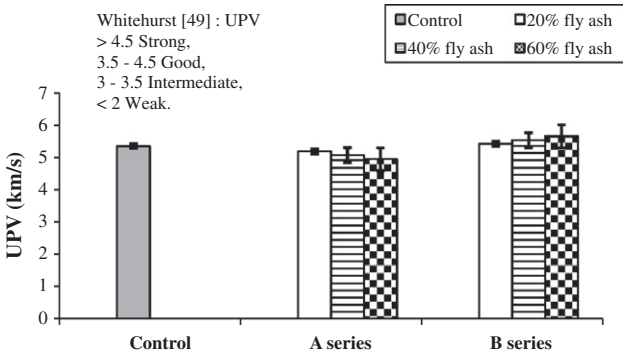

Fig. 11. UPV values of RCC mixtures.

the workability of fresh mixtures, consistent with the lower permeable voids content of mixture B3 in Fig. 5.

4.4. Dynamic elastic modulus determined by ultrasonic pulse velocity (UPV)

The 90-day UPV test results of RCC mixtures are presented in Fig. 11. Each value is the average of three measurements. The UPV of concrete is affected by a number of variables e.g., age, moisture condition, concrete porosity, aggregate type and ITZ characteristics. It can be seen that the UPV values of all RCC mixtures were higher than 4.5 km/s, the limit specified for strong concrete by Whitehurst [49]. The results indicate that in series A, UPV values were slightly decreased with increasing fly ash content and consequently increasing w/b ratio of the mixture. Since UPV value is a function of density and ITZ characteristics of the concrete [50,51], the reduction in UPV values of the series A mixtures is due to increasing porosity upon increasing w/b ratio of the mixture – increased from 0.39 (control mixture) to 0.46 (mixture where 60 wt.% of the cement is replaced with fly ash). However, in series B, UPV values were slightly increased with increasing fly ash content and w/b ratio of the mixture. This may be attributed to the better compactability of the series where aggregate was replaced with fly ash compared to that of the control mixture.

It is stated that the dynamic modulus of elasticity is generally 20%, 30%, and 40% higher than the static modulus of elasticity for high-, medium-, and low-strength concretes, respectively. The factors affecting dynamic modulus of elasticity of concrete are the properties of aggregate, cement paste and ITZ characteristics [11]. The aggregate content in typical RCC mixtures is higher than that of conventional concrete, thus the effect of aggregate characteristics on dynamic modulus of elasticity of RCC is of greater significance [52]. The dynamic modulus of elasticity vs. number of freeze–thaw cycles for RCC mixtures is summarized in Fig. 12. Each value represents the average of three measurements. It can be seen that at the beginning of the freeze–thaw cycles, i.e. 90-days, the dynamic elastic modulus of the series A mixtures was lower than that of control mixture in the range of 7–17%. This effect is due to the reduction of hardened concrete density with increasing fly ash content compared to that of the control mixture. However, in spite of reduction in aggregate content, the dynamic elastic modulus of series B mixtures at the beginning of freeze–thaw cycles was 1–3% greater than that of control mixture which may be considered as negligible. Thus, when even up to 20 wt.% of aggregate (corresponding to 60 wt.% of cement) is replaced with fly ash, the dynamic elastic modulus of the RCC remains about the same as that of control mixture. The effect of freeze–thaw cycles on dynamic elastic modulus is further discussed in Section 4.5.

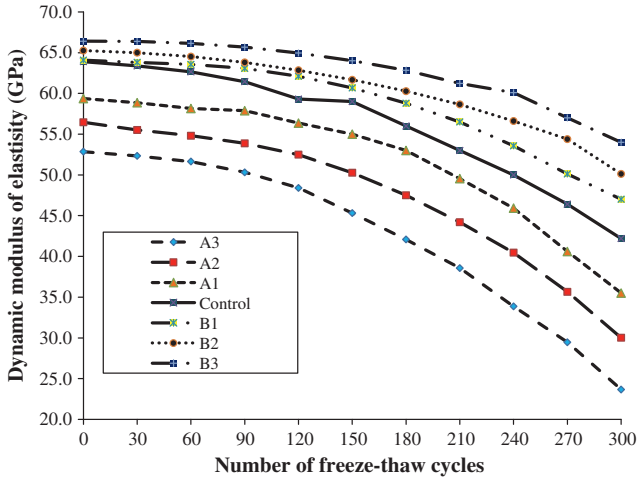

Fig. 12. Dynamic modulus of elasticity – number of freeze–thaw cycles of RCC mixtures.

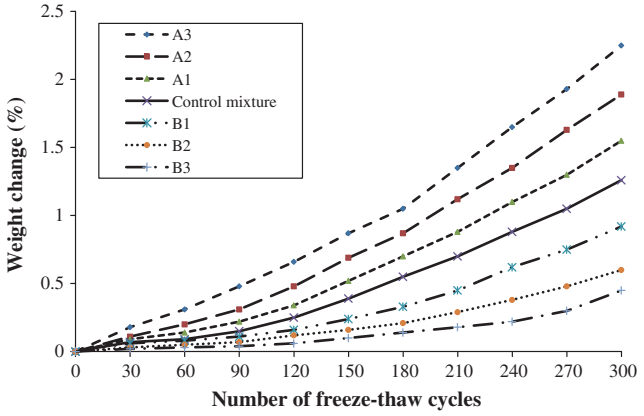

Fig. 13. Weight change percentage of RCC mixtures during freeze–thaw cycles.

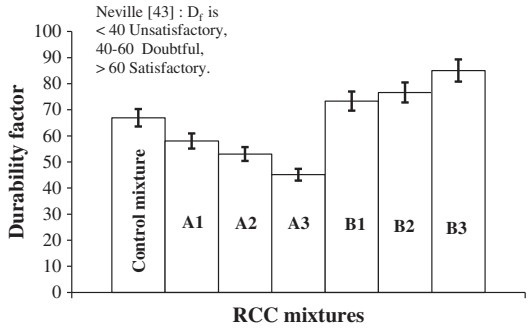

Fig. 14. Durability factor of RCC mixtures.

4.5. Freeze–thaw resistance

The change in the dynamic elastic modulus of RCC after 300 freeze–thaw cycles is shown in Fig. 12. It can be seen that the series A mixtures have shown more damage compared to series B mixtures. At the end of 300 freeze–thaw cycles the dynamic elastic modulus of series B mixtures was 10–26% greater than that of the control mixture. However, in series A mixtures at the end of same freeze–thaw cycles the dynamic elastic modulus was 20–45% lower than that of the control mixture.

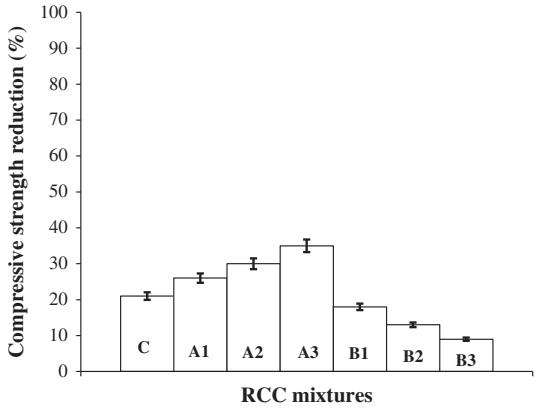

Fig. 15. Compressive strength reduction percentage of RCC mixtures after 300 freeze–thaw cycles.

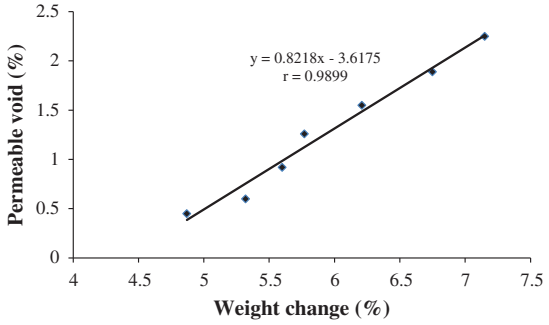

Fig. 16. Relationship between permeable voids and weight change percentages of RCC mixtures after 300 freeze–thaw cycles.

The weight change (at every 30 freeze–thaw cycles), durability factor, compressive strength reduction and relationship between weight change and permeable void content of RCC after 300 cycles of freezing and thawing for all series are shown in Figs. 13–16, respectively. Each value represents the average of three measurements. As shown in Fig. 13, the weight changes of all mixtures, not surprisingly, increased with an increase in the number of freeze–thaw cycles. Weight change increases of series A mixtures were higher than that of the control mixture, indicating that the series A specimens absorbed more water due to inferior transport properties compared to that of the control mixture. In other words, an increase in the w/b ratio increased the number and volume of the capillary pores as well as freezable water in the cement paste, which is the main cause of internal expansive pressure during freezing. However, the weight change of series B is lower than that of the control mixture. This may be attributed to the better compactability of series B compared to that of the control mixture.

As it can be seen from Fig. 14, the durability factor values of series B and control mixtures were higher than 60, the limit specified for satisfactory concrete as cited by Neville [43]. However, the durability factor values of series A were in the range of 40–60, the limit specified for doubtful concrete by the same reference. The resistance of the series B mixtures to freezing and thawing action is most likely due to an improved impermeability, which resulted from better compactability of series B compared to the other RCC mixtures.

Fig. 15 represents the compressive strength reduction of the RCC mixtures after exposure to 300 freeze–thaw cycles. Compared to the control mixture, the compressive strength loss increased for series A and decreased for series B, as the fly ash replacement level increased. It can be seen that the reduction of compressive strength upon 300 freeze–thaw cycles varies between 26% and 35% in the series A and between 9% and 18% in the series B. However, this reduction in the control mixture was 21%. It is clear that series B mixtures exhibited a much better resistance to repeated freeze–thaw cycles compared to other mixtures due to better compactability of this series. As expected, after 300 freeze–thaw cycles, a strong linear relationship was obtained between permeable void content and weight change percentages of the RCC mixtures.

5. Conclusion

For the materials used and test methods applied the following conclusions can be drawn:

- Compared to the control mixture, transport properties and freeze–thaw mass loss increased for the mixtures where cement was replaced with fly ash and decreased for the mixtures where aggregate was replaced with fly ash. The effect was more pronounced when the replacement level of fly ash increased.
- As it was proven that the 20 wt.% of aggregate replacement with fly ash was found to be effective by means of strength, durability and transport properties, this design approach may be preferable where fly ash and aggregate costs are similar to each other. Higher replacement levels should be further studied.
- The depth of penetration of water under pressure when the water penetration was parallel to the casting layers was always higher than that when the water penetration was perpendicular to the casting layers due to presence of cold joints between compaction layers.
- In spite of the reduction in aggregate content, the dynamic elastic modulus of the mixtures where aggregate was replaced with fly ash was not affected significantly compared to that of control mixture. This is consistent with the observation that the aggregate replacement with fly ash results in better compaction.
- Strong linear relationships were obtained between permeable void content – water absorption, and – weight change as well as depth of penetration of water under pressure, – permeable void content and – sorptivity values of the RCC mixtures.

Acknowledgements

The authors would like to thank Izmir Çimentaş cement plant authorities for their kind assistance in providing the cement and fly ash, as well as for determining the chemical compositions of these binders.

References

[1] Mardani-Aghabaglou A, Ramyar K. Mechanical properties of high-volume fly ash roller compacted concrete designed by maximum density method. Constr Build Mater 2013;38:356–64.
[2] Madhkhan M, Azizkhani R, Torki Harchegani ME. Effects of pozzolans together with steel and polypropylene fibers on mechanical properties of RCC pavements. Constr Build Mater 2012;26(1):102–12.
[3] Cao Ch, Sun W, Qin H. The analysis on strength and fly ash effect of roller compacted concrete with high volume fly ash. Cem Concr Res 2000;30(1):71–5.
[4] Atiş CD. Strength properties of high-volume fly ash roller compacted and workable concrete and influence of curing condition. Cem Concr Res 2005;35(6):1112–21.
[5] Chetan H, Halil C, Kejin W. Influences of mixture composition on properties and freeze–thaw resistance of RCC. Constr Build Mater 2011;25(1):313–9.
[6] Jittbodee Kh, Somnuk T. Vibration consistency prediction model for roller-compacted concrete. ACI Mater 2003;100(1):3–13.
[7] Andriolo FR. The use of roller compacted concrete. Brasil: Oficina de Textos; 1998.

[8] Hansen KD, Reinhardt WG. Roller compacted concrete dams. New York: McGraw-Hill; 1991.
[9] Pei-wei G, Sheng-xing W, Ping-hua L, Zhong-ru W, Ming-shu T. The characteristics of air void and frost resistance of RCC with fly ash and expansive agent. Constr Build Mater 2006;20(8):586–90.
[10] Amarnath Y, Ganesh Babu K. Transport properties of high volume fly ash roller compacted concrete. Cem Concr Compos 2011;33(10):1057–62.
[11] Mehta PK, Monteiro PJM. Concrete: microstructure, properties and materials. 3rd ed. McGraw- Hill; 2006.
[12] Nanni A. Abrasion resistance of roller compacted concrete. ACI Mater J 1989;86(6):559–65.
[13] Dolen TP. Freezing and thawing durability of roller-compacted concrete. ACI SPJ 1991;126(5):101–14.
[14] Mather B, Member H. Frost resistance of roller-compacted high-volume fly ash concrete. J Mater Civ Eng 1996;8(4):216.
[15] Ragan SA. Use of air entrainment to ensure the frost resistance of roller-compacted concrete pavements. ACI SPJ 1991;126(6):115–30.
[16] Pittman DW, Ragan SA. Drying shrinkage of roller-compacted concrete for pavement applications. ACI Mater J 1998;95(3):19–26.
[17] Delagrave A, Marchand J, Pigeon M, Boisvert J. Deicer salt scaling resistance of roller-compacted concrete pavements. ACI Mater J 1997;94(20):164–9.
[18] Li Z. Advanced concrete technology. 1st ed. Hoboken, New Jersey: Wiley; 2011.
[19] Nili M, Zaheri M. Deicer salt-scaling resistance of non-air-entrained roller-compacted concrete pavements. Constr Build Mater 2011;25(4):1671–6.
[20] Hazaree C, Ceylanb H, Wang K. Influences of mixture composition on properties and freeze–thaw resistance of RCC. Constr Build Mater 2011; 25(1):313–9.
[21] Gaoa PW, Wua SX, Lina PH, Wua ZR, Tang MS. The characteristics of air void and frost resistance of RCC with fly ash and expansive agent. Constr Build Mater 2006;20(8):586–90.
[22] Ghafoori N, Yuzheng C. Laboratory-made roller compacted concretes containing dry bottom ash: Part ii—long-term durability. ACI Mater J 1998;95(3):244–51.
[23] Hwang CL, Bui LAT, Lin KL, Lo CT. Manufacture and performance of lightweight aggregate from municipal solid waste incinerator fly ash and reservoir sediment for self-consolidating lightweight concrete. Cem Concr Compos 2012;34(10):1159–66.
[24] De la Varga I, Castro J, Bentz D, Weiss J. Application of internal curing for mixtures containing high volumes of fly ash. Cem Concr Compos 2012;34(9): 1001–8.
[25] Lopez-Calvo HZ, Montes-Garcia P, Bremner TW, Thomas MDA, Jiménez-Quero VG. Compressive strength of HPC containing CNI and fly ash after long-term exposure to a marine environment. Cem Concr Compos 2012;34(1):110–8.
[26] Tuyan M, Yazıcı H. Pull-out behavior of single steel fiber from SIFCON matrix. Constr Build Mater 2012;35:571–7.
[27] Şahmaran M, Özbay E, Yücel HE, Lachemi M, Li VC. Frost resistance and microstructure of engineered cementitious composites: influence of fly ash and micro poly-vinyl-alcohol fiber. Cem Concr Compos 2012;34(2):156–65.
[28] Boonserm K, Sata V, Pimraksa K, Chindaprasirt P. Improved geopolymerization of bottom ash by incorporating fly ash and using waste gypsum as additive. Cem Concr Compos 2012;34(7):819–24.
[29] Shuguang HU, Tingting Y, Fazhou W. Influence of mineralogical composition on the properties of lightweight aggregate. Cem Concr Compos 2010;32(1): 15–8.
[30] Şahmaran M, Özgür Yaman İ, Tokyay M. Transport and mechanical properties of self consolidating concrete with high volume fly ash. Cem Concr Compos 2009;31(2):99–106.
[31] EN 197-1. Cement – Part1: composition, specifications and conformity criteria for common cements. European Standard, Brussels; 2010.
[32] EN 450-1. Fly ash for concrete – Part 1: definition, specifications and conformity criteria. European standard, Brussels; 2008.
[33] EN 1097-6. Test for mechanical and physical properties of aggregates – Part 6: determination of particle density and water absorption. European Standard, Brussels; 2007.
[34] TS 802. Design of concrete mixtures. Ankara: Institute of Turkish Standards; 2009.
[35] ACI 207.5R-99. Roller-compacted mass concrete. Reported by ACI Committee 207; 1988.
[36] ASTM C 1435/C1435M-08. Standard practice for molding roller-compacted concrete in cylinder molds using a vibrating hammer. Annual book of ASTM Standards. Philadelphia, PA, USA: American Society for Testing and Materials; 2003.
[37] ASTM C 1170. Test methods for determining consistency and density of roller-compacted concrete using vibrating table. Annual book of ASTM Standards. Philadelphia, PA, USA: American Society for Testing and Materials; 1998.
[38] ASTM C 642-82. Standard test method for density, absorption and voids in hardened concrete. Annual book of ASTM Standards. Philadelphia, PA, USA: American Society for Testing and Materials; 1995.
[39] TS EN 12390-8. Testing hardened concrete – Part 8: depth of penetration of water under pressure. European standard, Brussels; 2009.
[40] EN 12390-7. Testing hardened concrete – Part 7: density of hardened concrete. European Standard, Brussels; 2010.
[41] ASTM C 1585. Standard test method for measurement of rate of absorption of water by hydraulic-cement concretes. Annual book of ASTM Standards. Philadelphia, PA, USA: American Society of Testing Materials; 2004.
[42] ASTM C 597. Standard test method for pulse velocity through concrete. Annual Book of ASTM Standards. Philadelphia, PA, USA: American Society of Testing Materials; 2002.
[43] Neville A. Concrete technology. 2nd ed. UK: Longman; 2010.
[44] Philleo R. Comparison of results of three methods for determining young's modulus of elasticity of concrete. J Am Concr Inst 1955;51(1):461–70.
[45] ASTM C 666/C666M-03. Standard test method for resistance of concrete to rapid freezing and thawing. Annual book of ASTM Standards. Philadelphia, PA, USA: American Society for Testing and Materials; 2008.
[46] TS 3699. Methods of testing for natural building stones. Ankara: Turkish Standard Institution; 1987 [in Turkish].
[47] CEB-FIP. Diagnosis and assessment of concrete structures – state of art report. CEB Bull 1989;192:83–5.
[48] Banthia N, Pigeon M, Marchand J, Boisvert J. Permeabılıty of roller compacted concrete. J Mater Civ Eng 1990;4(1):27–40.
[49] Whitehurst EA. Soniscope test concrete structure. J Am Concr Inst 1951;47:443–4.
[50] Lin Y, Lai CP, Yen T. Prediction of ultrasonic pulse velocity (UPV) in concrete. ACI Mater J 2003;100(1):21–8.
[51] Naik T, Malhotra VM, Popovics JS. The ultrasonic pulse velocity method. In: Malhotra VM, Carino NJ, editors. Handbook of nondestructive testing of concrete. CRC Press; 2004.
[52] Gauthier P, Marchand J. Design and Construction of Roller Compacted Concrete in Quebec, Canada; 2005. 111p.